

STUDY OF THE DEFECTIVE STRUCTURE OF LITHIUM NIOBATE CRYSTALS OF DIFFERENT COMPOSITIONS AND THEIR INFLUENCE ON THE OPTICAL AND ELECTRICAL PROPERTIES

N. V. Sidorov¹, N. A. Teplyakova^{1*},
and M. N. Palatnikov¹

The work considers the influence of various types of equilibrium defects on photovoltaic and diffusion fields and on the band gap of nominally pure and zinc-doped lithium niobate crystals. Concentrations of OH groups and point defects in the Nb_{Li} cationic sublattice (the deepest electron traps) and the Li/Nb ratio are calculated from the IR absorption spectra to estimate their contributions to proton conductivity. The IR absorption spectra reveal a correlation between the concentration of Nb_{Li} defect and the intensity of bands at ~3480 cm⁻¹.

DOI: 10.1134/S0022476621080059

Keywords: crystals, lithium niobate, doping, IR spectroscopy, photoelectric fields, defects, proton and polaron conductivity, band gap.

INTRODUCTION

Lithium niobate (LiNbO₃) is a heterodesmic nonlinear optical variable-composition crystal with a complex range of various types of defects (point and complex) possessing a number of unique physical properties. Constant interest to its study is due to wide applications of LiNbO₃ crystals in optical memory devices, electro-optical modulation and conversion, generation of optical harmonics, etc. Of considerable interest are comparative studies of optical and electrical characteristics of LiNbO₃ crystals within the practically important temperature range (near T_{room}) depending on the structure's composition and defectiveness. There are many uncertainties regarding the nature of the conductivity of LiNbO₃ crystals near T_{room} [1-6]. The character and quantitative parameters of conductivity in variable composition phases, including the LiNbO₃ crystal, are largely determined by characteristics of point defects in the cationic sublattice and by the charge carriers localized on these defects. It is therefore important to study the conductivity mechanisms in the structure of LiNbO₃ crystals of various compositions and genesis, namely, nominally pure structures with different Li/Nb ratios and doped structures with different degrees of defectiveness.

The electrical conductivity of LiNbO₃ crystals was studied mainly at relatively high temperatures in the region of predominant lithium ionic conductivity [1, 3, 7-11]. At near room temperature, the conductivity in LiNbO₃ crystals is of mixed ion-electronic nature (proton, polaron, or impurity hopping). The mechanism of impurity hopping conductivity is

¹Tananaev Institute of Chemistry and Technology – Kola Science Center, Russian Academy of Sciences, Apatity, Russia; *n.tepliakova@ksc.ru. Original article submitted December 14, 2020; revised April 1, 2021; accepted April 1, 2021.

typical of LiNbO_3 crystals containing sufficient amounts of multiply charged photorefractive cations (e.g. iron); in this case, conduction proceeds through Fe^{2+} - Fe^{3+} pairs [4]. The electrical conductivity of nominally pure crystals grown from charges of special purity and the conductivity of LiNbO_3 crystals doped with non-photorefractive cations of constant valence (Zn, Mg, etc) are mainly due to the contribution of small polarons $\text{Nb}_{\text{Li}}^{3+}$ [5]. The pyroelectric properties and conductivity of nominally pure LiNbO_3 samples with different Li/Nb ratios were studied at 290-450 K in [6]. It was shown that electronic contribution to the electrical conductivity decreases markedly in these crystals as their composition approaches the stoichiometric ratio ($\text{Li}/\text{Nb} = 1$) [6]. Strong anisotropy of electrical conductivity was reported in nearly stoichiometric LiNbO_3 crystals. The authors of [6] explain this fact by the changes in the properties of charge carriers: the proton contribution to electrical conductivity increases as the composition becomes more stoichiometric.

Supposedly, the nature of conductivity in the LiNbO_3 crystal is determined, among other factors, by point defects of the cation sublattice and by complex defects due to the localization of hydrogen bonds in the crystal. The niobium ion at lithium ion positions (Nb_{Li} defect) is the kind of point defect that leads to the formation of many other types of more complex defects in the LiNbO_3 crystal. The number of such defects in the structure of a nominally pure crystal is determined by its stoichiometry, and the perfectly stoichiometric crystal ($\text{Li}/\text{Nb} = 1$) should contain no Nb_{Li} defects. Consequently, the probability that hydrogen atoms in the LiNbO_3 crystal lattice are localized inside complex defects containing the Nb_{Li} point defect decreases [12], in some contradiction with conclusions of [6].

The number of Nb_{Li} defects in the congruent LiNbO_3 crystal ($\text{Li}/\text{Nb} = 0.946$) is $\sim 1 \text{ mol.}\%$. The Nb_{Li} defects have an effective charge of 4+ with respect to the lattice. The charge is compensated by other point defects, in particular, vacancies in lithium positions (V_{Li}^-) [13]. The Nb_{Li} defects are deep electron traps which form small polarons ($\text{Nb}_{\text{Li}}^{3+}$) and bipolarons ($\text{Nb}_{\text{Li}}^{3+}-\text{Nb}_{\text{Li}}^{4+}$) as a result of electron trapping [14]. In the temperature range from T_{room} and slightly above, the mechanism of polaron conductivity prevails [5]. Decreasing the crystal temperature to that of liquid nitrogen leads to the “freezing” of small polarons; as a result, the motion of Heitler–London bipolarons over vacant sites (complex defects ($\text{Nb}_{\text{Li}}^{4+}-\text{Nb}_{\text{Li}}^{5+}$)) becomes the main mechanism of electrical conductivity in the LiNbO_3 crystal [15]. Real stoichiometric crystals with small numbers of Nb_{Li} defects and, consequently, small polaron contribution to the conductivity have shallow electron traps (“sticking levels” near the bottom of the conduction band) whose formation mechanism is still unclear [16].

The ionic component of conductivity is due to lithium ions (Li^+) and protons (H^+). Hydrogen enters the LiNbO_3 crystal structure in an uncontrolled manner during the growth and post-growth processing and can occur in the crystal in the bound state (hydrogen bonding with oxygen) or in the form of interstitial protons H^+ . The amount of bound hydrogen depends on the composition of the LiNbO_3 crystal and on the method of its preparation and falls within a range of 10^{17} - 10^{19} cm^{-3} [12]. Assumingly, the concentration of interstitial protons H^+ increases together with the concentration of bound hydrogen in the crystal and with the degree of the crystal's imperfection. The Li^+ ionic conductivity occurs below 450 K with an activation energy of ~ 1.15 - 1.35 eV [7]. The Raman spectra (which provide important indirect data on conductivity) recorded for LiNbO_3 crystals of various compositions at 100-450 K showed that the widths of bands corresponding to Li^+ vibrations do not exhibit exponential behavior, which is characteristic of thermal activation mechanisms (jumps or reorientations of structural units between equilibrium positions); therefore, it was concluded that Li^+ cations do not contribute notably to the crystal's ionic conductivity at T_{room} [17]. Also, it was mentioned in [2] that oxygen vacancies (V_{O}) can possibly participate in the conduction with an activation energy of $\sim 1.3 \text{ eV}$.

In the present work, the IR absorption spectra in the region of OH^- stretchings are used to conduct comparative studies of hydrogen content and its relation to point defects in LiNbO_3 crystals of various compositions. The study aims at establishing the type of charge carriers responsible for the conductivity near T_{room} depending on the composition of the LiNbO_3 crystal and the imperfection degree of its structure. Nominally pure nearly stoichiometric crystals (crystal $\text{LiNbO}_{3\text{stoich}}$ (6.0 wt.% K_2O)) and congruent crystals ($\text{LiNbO}_{3\text{cong}}$) as well as doped $\text{LiNbO}_3:\text{Zn}$ crystals with a ZnO molar content of 0.04, 0.07, 1.19, 1.40, 2.01, 4.46, 4.54, 4.68, 6.50 were considered. The studied lithium niobate crystals differ as far as the number and type of point defects in the form of deep and shallow electron traps, deformation degree

(“perturbation”), doping addition of oxygen octahedra O₆ (determining their polarizability), ordering of structural units of the cationic sublattice along the polar axis, and, consequently, the band structure and electro-optical properties of the crystal. Since diffusion and the photovoltaic effect are the main factors of charge transfer in the undoped LiNbO₃ crystal, we estimated quantitatively photovoltaic and diffusion fields as well as band gaps for all studied crystals.

EXPERIMENTAL

Crystals LiNbO₃_{cong}, LiNbO₃:Zn (0.04-6.50 mol.% ZnO) were prepared from a congruent melt using a standard technique [18]. The lithium niobate charge of congruent composition (48.6 mol.% Li₂O) was prepared in the Tananaev Institute of Chemistry and Technology by the method of granulation synthesis [19]. The dopant concentration in the crystals was determined by the electron microprobe analysis. The nearly stoichiometric LiNbO₃_{stoich} crystal (6.0 wt.% K₂O) was prepared using high temperature top speed solution growth (HTTSSG) [12, 18-20] from a congruent melt with an addition of 6 wt.% potassium oxide flux. The technological regimes of growing nominally pure and doped lithium niobate crystals are described in more detail in [20].

The grown crystals were monodomainized by high-temperature electrodiffusion annealing in a LANTAN installation. The degree of monodomainization was estimated by analysing the static piezoelectric effect [21, 22].

The IR absorption spectra were registered on a Bruker IFS 66 v/s spectrometer. The band gap was determined by recording the transmission spectra of the crystals on an MDR-41 monochromator. Photo-induced light scattering (PILS) in the crystals was registered on a setup described in [23] using a MLL-100 Nd:YAG laser ($\lambda = 532$ nm, $p \sim 6.3$ W/cm²) was used. The kinetic dependencies of the photorefractive effect and photoelectric fields (photovoltaic and diffusion) were studied by the interference-polarization method on a setup described in [24] using a Spectra Physics 2018-RM laser ($\lambda = 514.5$ nm, $P = 282$ mW). The photovoltaic and diffusion fields were calculated according to the equations proposed in [25]. The refractive indices of extraordinary and ordinary beams were determined from empirical equations reported in [26].

RESULTS AND DISCUSSION

Exposing the photorefractive LiNbO₃ crystal to laser irradiation causes photoinduced light scattering by static and fluctuating defects with a modified laser-induced refractive index [27, 28]. Fig. 1 shows the PILS images of studied LiNbO₃ crystals of various compositions. The Table 1 lists calculated values of PILS opening angles, photovoltaic E_{PV} and diffusion E_D fields, and band gaps of LiNbO₃ crystals of various compositions. It is known that photovoltaics is the main photorefractive mechanism in the crystal LiNbO₃ [13, 29, 30]. In this case, the magnitude of the electro-optical effect determines the PILS opening angle (θ , deg) [27, 28], while the indicatrix opening velocity and angle θ affect the speed of photorefractive data record and the speed of optical shutter in lithium niobate crystals [28, 31].

On the other hand, the properties of crystal LiNbO₃ can be brought closer to those of semiconductors by decreasing the band gap as a result of doping and creating new energy levels, which allows developing novel ferroelectric materials with cross-effects.

As can be seen from the Table 1, the strongest photovoltaic fields are observed in crystals LiNbO₃_{cong}, LiNbO₃:Zn (0.07 mol.%, 4.46 mol.%, 4.54 mol.%, 6.50 mol.% ZnO) where no PILS occurs at the utilized laser power (Fig. 1). Note that crystals LiNbO₃_{stoich} (6.0 wt.% K₂O) and LiNbO₃:Zn (0.04 mol.%, 1.19 mol.%, 1.40 mol.%, 2.01 mol.% ZnO) exhibiting PILS indicatrix opening (Fig. 1) have stronger diffusion fields and smaller band gaps (see the Table 1).

In nominally pure crystals LiNbO₃_{cong} and in LiNbO₃ crystals doped with non-photorefractive impurities (in particular, LiNbO₃:Zn crystals), the Nb_{Li} defects are deep electronic traps [13, 29] ensuring polaron conductivity [15]. According to the model of Nb_{Li}⁴⁺ defect compensation by Li vacancies (V_{Li}^-) [13], the concentration of Nb_{Li}⁴⁺ point defects in the structure of nominally pure LiNbO₃ crystals can be calculated according to the following equations [32]:

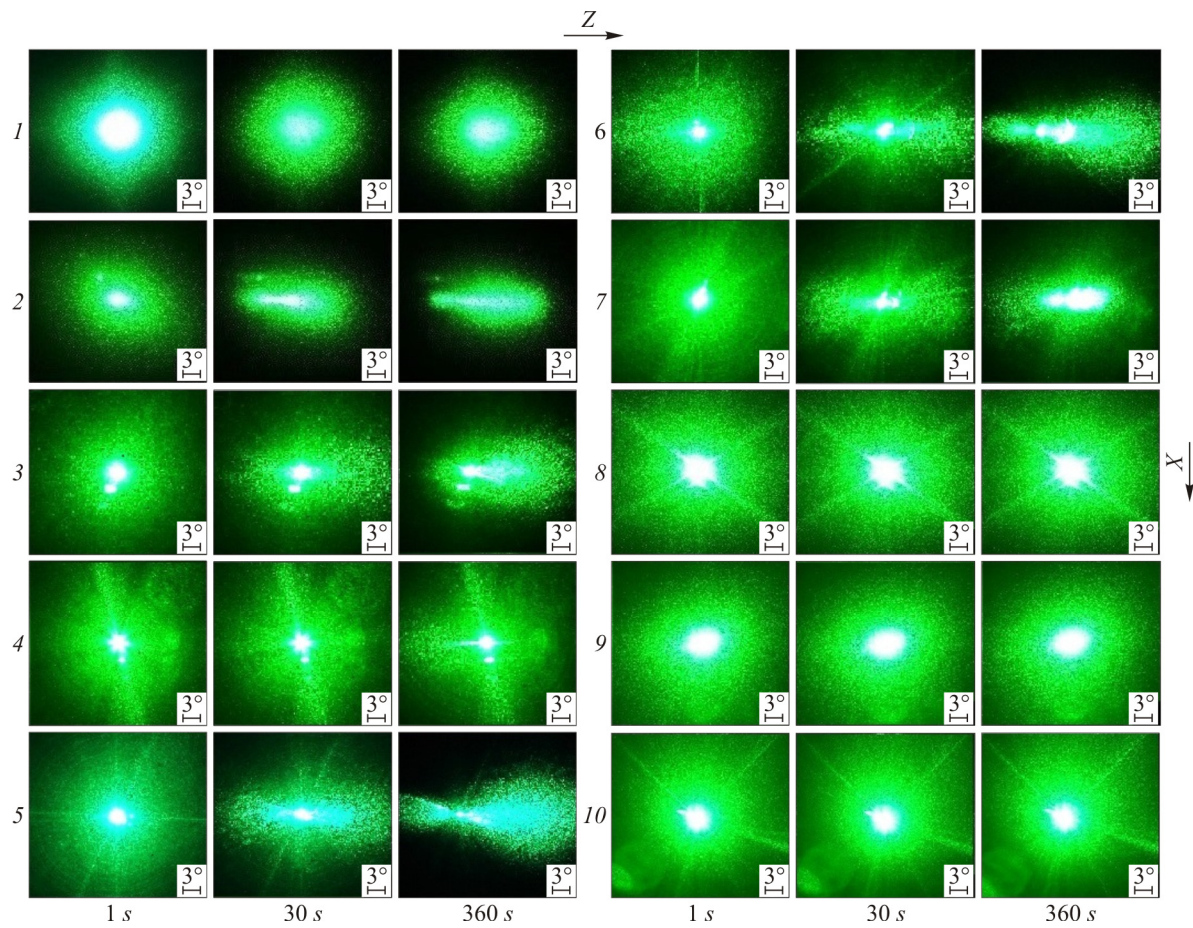


Fig. 1. PILS images of crystals $\text{LiNbO}_3^{\text{cong}}$ (1), $\text{LiNbO}_3^{\text{stoich}}$ (6.0 wt.% K_2O) (2), $\text{LiNbO}_3:\text{Zn}$ (0.04) (3), $\text{LiNbO}_3:\text{Zn}$ (0.07) (4), $\text{LiNbO}_3:\text{Zn}$ (1.19) (5); $\text{LiNbO}_3:\text{Zn}$ (1.40) (6); $\text{LiNbO}_3:\text{Zn}$ (2.01) (7); $\text{LiNbO}_3:\text{Zn}$ (4.46) (8); $\text{LiNbO}_3:\text{Zn}$ (4.54) (9); $\text{LiNbO}_3:\text{Zn}$ (6.50 mol.% ZnO) (10); $\lambda = 532 \text{ nm}$, $p \sim 6.3 \text{ W/cm}^2$.

TABLE 1. Photovoltaic PILS Parameters, Band Gaps, Li/Nb Ratios, Concentrations of OH Groups ($\text{C(OH}^-)$), Numbers of Point Defects Nb_{Li} and V_{Li} in Lithium Niobate Crystals at T_{room}

Crystal	E , eV	E_{pv} , kV/cm	E_D , kV/cm	θ , deg	V_{Li} , mol.%	Nb_{Li} , mol.%	Li/Nb	C(OH)^- , cm $^{-3}$
$\text{LiNbO}_3^{\text{stoich}}$ (6.0 wt.% K_2O)	3.379	6.855	2.508	46	0.60	0.15	0.991	$4.03 \cdot 10^{16}$
$\text{LiNbO}_3^{\text{cong}}^{\#1}$	3.780	6.232	0.81	—	3.64	0.91	0.946	$8.15 \cdot 10^{16}$
$\text{LiNbO}_3:\text{Zn}$ (0.04)	3.685	4.82	1.256	18	3.24	0.81	0.952	$1.52 \cdot 10^{17}$
$\text{LiNbO}_3:\text{Zn}^{\#1}$ (0.07)	3.659	6.075	0.65	—	4.88	1.22	0.928	$1.55 \cdot 10^{17}$
$\text{LiNbO}_3:\text{Zn}$ (1.19)	3.609	4.73	2.313	23	2.68	0.67	0.960	$1.65 \cdot 10^{17}$
$\text{LiNbO}_3:\text{Zn}$ (1.40)	3.626	8.203	1.159	16.5	2.16	0.54	0.968	$1.44 \cdot 10^{17}$
$\text{LiNbO}_3:\text{Zn}$ (2.01)	3.632	4.783	1.384	20	2.16	0.54	0.968	$1.58 \cdot 10^{17}$
$\text{LiNbO}_3:\text{Zn}^{\#1}$ (4.46)	4.001	6.551	0.491	—	3.60	0	0.928	$2.66 \cdot 10^{16}$
$\text{LiNbO}_3:\text{Zn}^{\#1}$ (4.54)	3.953	6.823	0.22	—	2.40	0	0.952	$2.66 \cdot 10^{16}$
$\text{LiNbO}_3:\text{Zn}^{\#1}$ (6.50 mol.%)	3.950	7.721	0.48	—	1.35	0	0.973	$4.00 \cdot 10^{16}$

^{#1} No indicatrix opening occurs in these crystals at $p \sim 6.3 \text{ W/cm}^2$.

$$C(V_{Li}) = 100 \left(\frac{4 - 4(Li/Nb)}{5 + Li/Nb} \right), \quad (1)$$

$$C(Nb_{Li}) = C(V_{Li}) / 4. \quad (2)$$

The concentration of point defects in the structure of heavily doped $\text{LiNbO}_3:\text{Zn}$ crystals (4.46-6.50 mol.% ZnO) was calculated by equations proposed in [32] for magnesium doped crystals at concentrations above the threshold value (5.5 mol.% MgO):

$$C(V_{Li}) = 100 \left(\frac{1 - 4(Li/Nb)}{2} \right), \quad (3)$$

$$C(Nb_{Li}) = 0. \quad (4)$$

The Li/Nb ratio was determined from IR absorption spectra using procedure proposed in [32]. The calculated Li/Nb ratios and numbers of Nb_{Li} and V_{Li}^- defects are summarized in the Table 1. The highest concentration of Nb_{Li} defects is observed in crystals $\text{LiNbO}_{3\text{cong}}$ and $\text{LiNbO}_3:\text{Zn}$ (0.07 mol.% ZnO), which is the closest one to the congruent composition, while the lowest concentration is observed in the $\text{LiNbO}_{3\text{stoich}}$ crystal (6.0 wt.% K₂O). The structure of heavily doped crystals $\text{LiNbO}_3:\text{Zn}$ (4.46-6.50 mol.% ZnO) contains no point defects Nb_{Li} [29]. The obtained data indicate that polaron contribution to conductivity is significant in the lithium niobate crystal of congruent composition and in $\text{LiNbO}_3:\text{Zn}$ crystals (0.04-2.01 mol.% ZnO) with a relatively low dopant content. As the content of zinc increases, the concentration of Nb_{Li} defects in the structure of crystals $\text{LiNbO}_3:\text{Zn}$ decreases, while the photoelectric fields and PILS opening angles depend ambiguously on zinc concentration (see the Table 1).

The number of Nb_{Li} defects can be estimated also from the IR absorption spectra in the region of hydrogen bond stretchings (3420-3550 cm⁻¹). Fig. 2 shows the IR absorption spectra in the studied LiNbO_3 crystals of various compositions. The band at 3465 cm⁻¹ is considered to be characteristic of the structure of a highly perfect stoichiometric lithium niobate crystal where hydrogen atoms occupy only one position [12, 33]. The band at 3480 cm⁻¹ is characteristic of the lithium niobate crystal of congruent composition and is assigned to hydrogen bond stretchings in the $V_{Li}-\text{OH}$ complex [34]. The authors of [35, 36] proposed a method to calculate the Li/Nb ratio from the intensity ratio $I_{\text{rel}} = I_{3480}/I_{3465}$. This intensity ratio of bands at 3480 cm⁻¹ and 3465 cm⁻¹ decreases almost linearly with increasing Li/Nb value [35, 36]. Since the structure of crystal $\text{LiNbO}_{3\text{cong}}$ differs from that of crystal $\text{LiNbO}_{3\text{stoich}}$ by the presence of Nb_{Li} defects, we plotted the intensity of the band at 3480 cm⁻¹ as a function of the calculated number of Nb_{Li}^{4+} defects (Fig. 3). Fig. 3 shows that the concentration behavior of the band intensity at 3480 cm⁻¹ correlates well with the calculated number of Nb_{Li} defects independently on the crystal composition, with the exception of $\text{LiNbO}_3:\text{Zn}$ crystals (4.46-6.50 mol.% ZnO). The authors of method [32] (utilized in the present work to calculate the Nb_{Li} defects) assume that the structure of heavily doped crystals contains no point defects Nb_{Li}^{4+} . However, the analysis of Fig. 3 shows that the intensity of the band at 3480 cm⁻¹ in crystals $\text{LiNbO}_3:\text{Zn}$ (4.46-6.50 mol.% ZnO) is not zero. Apparently, the structure of crystals $\text{LiNbO}_3:\text{Zn}$ (4.46-6.50 mol.% ZnO) contains Nb_{Li} defects. This assumption is confirmed by the results reported in [37]: according to the full-profile XRD data, the structure of heavily doped crystals $\text{LiNbO}_3:\text{Zn}$ (4.76-5.19 mol.% ZnO) contains Nb_{Li}^{4+} defects.

The content of hydrogen atoms in the structure of the crystals was determined using the IR absorption spectra in the region of hydrogen bond stretchings. As hydrogen bonding is formed, the wave functions describing the electron orbitals of oxygen ions and their electron polarizability values are changed significantly while the NbO₆ octahedra, determining optical and electrical properties of LiNbO_3 crystal, are distorted [38, 39]. The Table 1 lists the concentrations of OH⁻ groups calculated from the IR absorption spectrum according to the method proposed in [40] for the studied LiNbO_3 crystals.

As can be seen from the Table 1, the lowest number of OH⁻ groups is observed in the $\text{LiNbO}_{3\text{stoich}}$ crystal (6.0 wt.% K₂O) and in heavily doped crystals $\text{LiNbO}_3:\text{Zn}$ (4.46-6.50 mol.% ZnO). It can be assumed that decreasing the number of bound OH⁻ groups increases the number of interstitial protons in heavily doped $\text{LiNbO}_3:\text{Zn}$ crystals, thus possibly enhancing

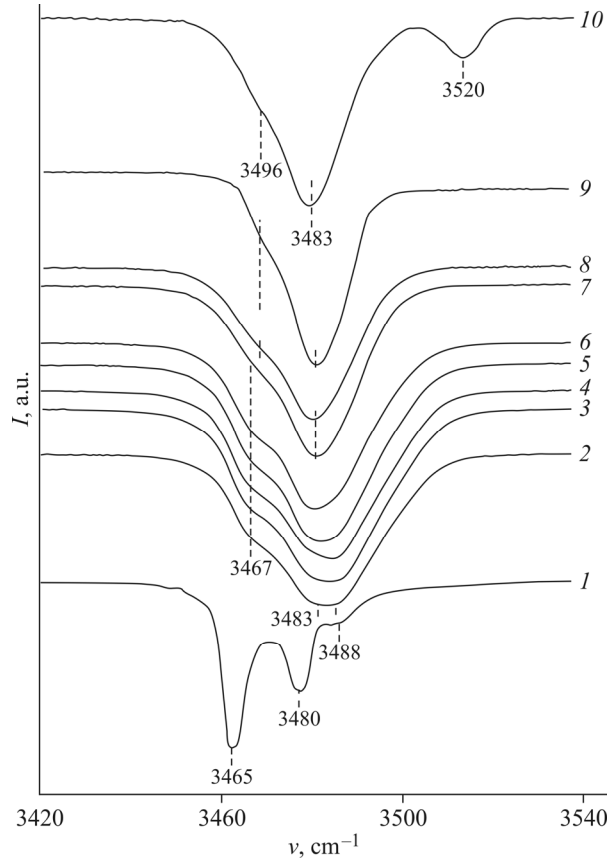


Fig. 2. IR absorption spectra in the region hydrogen bond stretchings in crystals $\text{LiNbO}_3\text{stoich}$ (6.0 wt.% K_2O) (1), $\text{LiNbO}_3\text{cong}$ (2), $\text{LiNbO}_3:\text{Zn}$ (0.04) (3); $\text{LiNbO}_3:\text{Zn}$ (0.07) (4); $\text{LiNbO}_3:\text{Zn}$ (1.19) (5); $\text{LiNbO}_3:\text{Zn}$ (1.40) (6); $\text{LiNbO}_3:\text{Zn}$ (2.01) (7); $\text{LiNbO}_3:\text{Zn}$ (4.46) (8); $\text{LiNbO}_3:\text{Zn}$ (4.54) (9); $\text{LiNbO}_3:\text{Zn}$ (6.50 mol.% ZnO) (10).

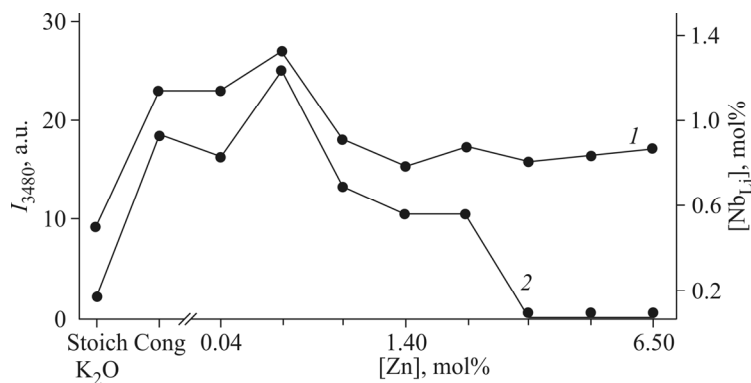


Fig. 3. Intensity of the IR absorption band at $3480\text{-}3483\text{ cm}^{-1}$ in the region of OH stretchings (1) and concentration of Nb_{Li} point defects (2) as functions of the composition of LiNbO_3 crystals: $\text{LiNbO}_3\text{stoich}$, $\text{LiNbO}_3\text{cong}$, $\text{LiNbO}_3:\text{Zn}$ (0.04–6.5 mol.% ZnO).

the proton conductivity and the rate of thermal fixation of holograms in these crystals compared to the $\text{LiNbO}_3\text{cong}$ crystal [13, 29]. The electrical conductivity of nearly stoichiometric crystals $\text{LiNbO}_3\text{stoich}$ (6.0 wt.% K_2O) also exhibit sharply lower electronic contribution and increased proton contribution [6]. At the same time, none of the studied lithium niobate crystals showed strong correlation between the Li/Nb ratio and the content of OH^- groups in crystals (see the Table 1); therefore, no

unambiguous conclusions can be drawn concerning direct relationship between proton conductivity and the Li/Nb value. Apparently, proton conductivity is determined, in addition to they Li/Nb ratio, by the nature of O–H bonds in various types of defective centers formed by hydrogen in the structure of crystals of lithium niobate of various compositions.

In strictly stoichiometric LiNbO_3 crystals, hydrogen atoms are more ordered, since hydrogen bonds are formed with only one oxygen ion (the one located on the polar axis Z) of the NbO_6 octahedron [38]. Thus, the highly ordered structure of the stoichiometric crystal contains only one position for the hydrogen atom and one IR absorption band in the frequency range $3420\text{--}3550\text{ cm}^{-1}$ [12, 38]. The presence of several positions of hydrogen atoms in the structure of nonstoichiometric LiNbO_3 crystals is clearly manifested in the IR absorption spectrum in the region of hydrogen bond stretchings. The spectrum of such crystals contains several bands corresponding to these positions. Crystal $\text{LiNbO}_{3\text{stoich}}$ (6.0 wt.% K_2O) also exhibits several absorption bands, indicating that the structure of this crystal does not completely correspond to the structure of a highly perfect strictly stoichiometric crystal. Nevertheless, Fig. 2 shows that the widths of all IR absorption bands the $\text{LiNbO}_{3\text{stoich}}$ (6.0 wt.% K_2O) crystal are much narrower than those in all other studied crystals, meaning that the structure of this crystal has a higher degree of order of hydrogen atoms.

The hydrogen atoms in the structure of crystals $\text{LiNbO}_{3\text{cong}}$ and $\text{LiNbO}_3:\text{Zn}$ can be localized in three different positions within complex defects $\text{Me}-\text{OH}$ and $\text{Me}-\text{OH}-\text{Me}(V_{\text{Li}})$ (Me is an impurity cation (Zn) or the main cation (Li, Nb)) [39]. The presence of such complex defects can affect positions of energy levels localized in the band gap and lead to the formation of new levels.

CONCLUSIONS

Thus, heavily doped crystals $\text{LiNbO}_3:\text{Zn}$ (4.46–6.50 mol.% ZnO) exhibited increased band gaps and a noticeably decreased concentrations of OH groups. The structure of heavily doped crystals $\text{LiNbO}_3:\text{Zn}$ (4.46–6.50 mol.% ZnO) clearly show increase in the number of interstitial protons and, consequently, stronger proton conductivity. Weakly doped crystals $\text{LiNbO}_3:\text{Zn}$ (0.04–2.01 mol.% ZnO) demonstrate no correlation between concentrations of OH^- groups, magnitudes of photovoltaic fields, band gap values, PILS opening angles, and Li/Nb ratios. Therefore, the localization features of hydrogen atoms in the structure of lithium niobate crystals of various compositions should be taken into account when estimating the proton conductivity. In the nearly stoichiometric crystal $\text{LiNbO}_{3\text{stoich}}$ (6.0 wt.% K_2O), hydrogen atoms form hydrogen bonds mainly with one of the oxygen ions of the NbO_6 octahedron; as a result, these oxygen octahedra are strongly distorted, the band gap diminishes, and the contribution to the proton conductivity increases. In the structure of $\text{LiNbO}_3:\text{Zn}$ crystals, hydrogen atoms are part of complex defects $\text{Me}-\text{OH}$ and $\text{Me}-\text{OH}-\text{Me}(V_{\text{Li}})$ (Me is an impurity cation or the main cation) and do not have such a noticeable effect on the distortion of NbO_6 octahedra, band gap decrease, and increase in the contribution to proton conductivity as in nominally pure crystals $\text{LiNbO}_{3\text{stoich}}$ (6.0 wt.% K_2O). The calculated number of Nb_{Li} defects correlates with the intensity of the IR absorption band at $\sim 3480\text{ cm}^{-1}$. Obviously, this allows estimating comparative concentrations of Nb_{Li} point defects in lithium niobate crystals of various compositions in the cases when calculating the number of Nb_{Li} defects is complicated, e.g., for heavily doped crystals $\text{LiNbO}_3:\text{Me}$ ($\text{Me} = \text{Zn}, \text{Mg}$, etc.).

CONFLICT OF INTERESTS

The authors declare that they have no conflict of interests.

REFERENCES

1. A. A. Esin, A. R. Akhmatkhanov, and V. Ya. Shur. *Ferroelectrics*, **2016**, *496*, 102, DOI: 10.1080/00150193.2016.1157438.
2. A. S. Pritulenko, A. V. Yatsenko, and S. V. Yevdokimov. *Crystallogr. Rep.*, **2015**, *60*, 267, DOI: 10.1134/S1063774515020224.

3. R. Bhatt, S. Ganesamoorthy, I. Bhaumik, A. K. Karnal, and P. K. Gupta. *J. Phys. Chem. Solids*, **2012**, *73*, 257, DOI: 10.1016/j.jpcs.2011.10.033.
4. Y. Yang, I. Nee, K. Buse, and D. Psaltis. *Appl. Phys. Lett.*, **2001**, *78*, 4076.
5. O. F. Shirmer, M. Imlau, C. Merschjan, and B. Schoke. *J. Phys. Condens. Matter*, **2009**, *21*, 123201, DOI:10.1088/0953-8984/21/12/123201.
6. A. V. Yatsenko, S. V. Yevdokimov, M. N. Palatnikov, N. V. Sidorov. *Phys. Solid State*, **2019**, *61*, 1211, DOI: 10.1134/S106378341907031X and.
7. A. El-Bachiri, F. Bennani, and M. Bousselamti. *Spectrosc. Lett.*, **2014**, *47*, 374, DOI: 10.1080/00387010.2013.857356.
8. G. Mandula, K. Lengyel, L. Kovacs, M. Ellaban, R. A. Rupp, and M. Fally. *SPIE Proc.*, **2001**, *4412*, 226, DOI: 10.1117/12.435830.
9. K. Lengyel, L. Kovacs, G. Mandula, and R. A. Rupp. *Ferroelectrics*, **2001**, *257*, 255, DOI: 10.1080/00150190108016307.
10. G. Ohlendorf, D. Richter, J. Sauerwald, and H. Fritze. *Diffus. Fundam.*, **2008**, *8*, 6.1.
11. C. H. Swanson, M. Schulz, H. Fritze, J. Shi, K.-D. Becker, P. Fielitz, and G. Borchardt. *Diffus. Fundam.*, **2010**, *12*, 48.
12. K. Lengyel, A. Peter, L. Kovacs, G. Corradi, L. Palfavi, J. Hebling, M. Unferdorben, G. Dravecz, I. Hajdara, Zs. Szaller, and K. Polgar. *Appl. Phys. Rev.*, **2015**, *2*, 040601, DOI: 10.1063/1.4929917.
13. N. V. Sidorov, T. R. Volk, B. N. Mavrin, and V. T. Kalinnikov. Niobat litiya. Defekty, Fotorefrakt., Kolebat. Spektr. Polyar. (Lithium Niobate: Defects, Photorefraction, Vibrational Spectra, Polaritons) [in Russian]. Nauka: Moscow, **2003**.
14. O. Schirmer, O. Thieman, and M. Wöhlecke. *J. Phys. Chem. Solids*, **1991**, *52*, 185, DOI: 10.1016/0022-3697(91)90064-7.
15. I. Sh. Akhmadullin, V. A. Golenishchev-Kutuzov, and S. A. Migachev. *Phys. Solid State*, **1998**, *40*, 1012, DOI: 10.1134/1.1130478.
16. A. A. Blistanov, V. M. Lubchenko, and A. N. Gorjunova. *Kristallographija*, **1998**, *43*, 86. (In Russ.)
17. N. V. Sidorov, A. A. Kruk, A. A. Yanichev, M. N. Palatnikov, and B. N. Mavrin. *Opt. Spectrosc.*, **2014**, *117*, 560, DOI: 10.1134/S0030400X14100208.
18. M. N. Palatnikov, I. V. Birukova, S. M. Masloboeva, O. V. Makarova, D. V. Manukovskaya, and N. V. Sidorov. *J. Cryst. Growth.*, **2014**, *386*, 113, DOI: 10.1016/j.jcrysgr.2013.09.038.
19. M. N. Palatnikov, N. V. Sidorov, I. V. Birukova, O. B. Shcherbina, and V. T. Kalinnikov. *Perspekt. Mater.*, **2011**, *2*, 93.
20. M. N. Palatnikov, N. V. Sidorov, O. V. Makarova, and I. V. Birukova. Fundam. Aspeky Tehnol. Silno Legir. Kristall. Niobata Litiya (Fundam. Aspects Technol. Heavily Doped Lithium Niobate Cryst.) [in Russian]. Publishing House of the KSC RAS: Apatity, **2017**
21. M. N. Palatnikov, V. A. Sandler, N. V. Sidorov, I. N. Efremov, and O. V. Makarova. *Instrum. Exp. Tech.*, **2020**, *63*, 383, DOI: 10.1134/S002044120040089.
22. M. N. Palatnikov, V. A. Sandler, N. V. Sidorov, I. N. Efremov, and O. V. Makarova. *Inorg. Mater.*, **2020**, *56*, 1153, DOI: 10.1134/S0020168520110126.
23. N. V. Sidorov, O. Yu. Pikoul', N. A. Teplyakova, and M. N. Palatnikov. Laser. Konoskop. Fotoindut. Rassey. Svet. Issled. Svoistv Nelin.-Optic. Krist. Niobata Litiya (Laser Conoscop. Photoinduc. Light Scatt. Res. Prop. Optic. Nonlinear Lithium Niobate Cryst.) [in Russian]. RAS: Moscow, **2019**.
24. A. V. Syuy, A. A. Gabain, N. A. Teplyakova, N. V. Sidorov, and M. N. Palatnikov. *Prib. Tekh. Eksp.*, **2017**, *6*, 134, DOI: 10.7868/S003281621706012X.
25. M. Goulkov, M. Imlau, and Th. Woike. *Phys. Rev. B*, **2008**, *77*, 235110-1, DOI: 10.1103/PhysRevB.77.235110.
26. G. G. Gurzadyan, V. G. Dmitriev, and D. N. Nikoghosyan. Nelin.-Optic. Kristall. Svoistv. Primenen. Kvant. Electron. (Nonlinear Opt. Cryst. Prop. Appl. Quantum Electron.) [in Russian]. Radio i Svyaz': Moscow, **1991**.)

27. V. V. Obukhovsky. Proces. Fotorefrakt. Rasseyan. Svet. Krist. (Proc. Light Scatt. Cryst.): Doctoral (Phys.-Math.) Dissertation [in Russian]. Kiev Gos. Univ.: Kiev, **1989**.
28. V. A. Maksimenko, A. V. Syuy, and Yu. M. Karpets. Fotoindut. Proc. Krist. Niobata Litiya (Photoinduc. Proc. Lithium Niobate Cryst.) [in Russian]. Fizmatlit: Moscow, **2008**.
29. T. Volk, M. Wöhlecke. Lithium niobate. Defects, Photorefraction and Ferroelectric Switching. Berlin: Springer, **2008**.
30. M. E. Lines and A. M. Glass. Princ. Appl. Ferroelectr. Relat. Mater. Clarendon Press, **1977**.
31. S. G. Odulov, M. S. Soskin, and A. I. Khizhnyak. Laser. Dynamic. Reshet. (Dynamic Grating Lasers) [in Russian]. Nauka: Moscow, **1990**.
32. M. Y. Salloum, O. S. Grunsky, A. A. Man'shina, A. S. Tver'yanovich, and Yu. S. Tver'yanovich. *Russ. Chem. Bull.*, **2009**, 58, 2228, DOI: 10.1007/s11172-009-0310-1.
33. K. Polgar, A. Peter, L. Kovacs, G. Corradi, and Zs. Szaller. *J. Cryst. Growth*, **1997**, 177, 211, DOI: 10.1016/S0022-0248(96)01098-6.
34. N. Iyi, K. Kitamura, F. Izumi, J. K. Yamamoto, T. Hayashi, H. Asano, and S. Kimura. *J. Solid State Chem.*, **1992**, 101, 340, DOI: 10.1016/0022-4596(92)90189-3.
35. G. Dravecz and L. Kovács. *Appl. Phys. B: Lasers Opt.*, **2007**, 88, 305, DOI: 10.1007/s00340-007-2704-9.
36. G. Dravecz, L. Kovács, A. Peter, K. Polgar, and P. Bourson. *Phys. Status Solidi C*, **2007**, 4, 1313, DOI: 10.1002/pssc.200673733.
37. N. V. Sidorov, N. A. Teplyakova, A. A. Yanichev, M. N. Palatnikov, O. V. Makarova, L. A. Aleshina, and A. V. Kadetova. *Inorg. Mater.*, **2017**, 53, 489, DOI: 10.1134/S002016851705017X.
38. S. V. Yevdokimov and A. V. Yatsenko. *Crystallogr. Rep.*, **2003**, 48, 542, DOI: 10.1134/1.1595175.
39. J. M. Cabrera, J. Olivares, M. Carrascosa, J. Rams, R. Müller, and E. Diéguez. *Adv. Phys.*, **1996**, 45, 349, DOI: 10.1080/00018739600101517.
40. S. Klauer, M. Wöhlecke, and S. Kapphan. *Phys. Rev. B*, **1992**, 45, 2786, DOI: 10.1103/PhysRevB.45.2786.